Aza Cope Rearrangement of Propargyl Enammonium Cations Catalyzed By a Self-Assembled \`Nanozyme

Hastings, Courntey J.

2009-07-28

Aza Cope Rearrangement of Propargyl Enammonium Cations Catalyzed By a Self-Assembled "Nanozyme"

Courtney J. Hastings, Dorothea Fiedler, Robert G. Bergman, Kenneth N. Raymond**

Contribution from the Department of Chemistry, University of California and Lawrence Berkeley National Laboratory

Berkeley, California, 94720

E-mail: rbergman@berkeley.edu; raymond@socrates.berkeley.edu

Abstract: The tetrahedral $[Ga_4L_6]^{12-}$ assembly (L = *N,N*-bis(2,3-dihydroxybenzoyl)-1,5-diaminonaphthalene) encapsulates a variety of cations, including propargyl enammonium cations capable of undergoing the aza Cope rearrangement. For propargyl enammonium substrates that are encapsulated in the $[Ga_4L_6]^{12-}$ assembly, rate accelerations of up to 184 are observed when compared to the background reaction. After rearrangement, the product iminium ion is released into solution and hydrolyzed allowing for catalytic turnover. The activation parameters for the catalyzed and uncatalyzed reaction were determined, revealing that a lowered entropy of activation is responsible for the observed rate enhancements. The catalyzed reaction exhibits saturation kinetics; the rate data obey the Michaelis-Menten model of enzyme kinetics, and competitive inhibition using a non-reactive guest has been demonstrated.

Introduction

In nature, enzymes utilize steric confinement and carefully-positioned functional groups to catalyze reactions with high degrees of activity and selectivity.[1-4] The extraordinary efficiency of enzymes under mild physiological conditions has challenged chemists to design enzyme mimics with the goals of achieving useful catalytic processes and furthering our understanding of enzymes. To emulate this mode of catalysis, many research groups have designed synthetic hosts capable of binding and directing the reactivity of guest molecules.[5-13] Upon encapsulation in either a synthetic host or an enzyme active site, the environment surrounding a guest molecule drastically differs from that of the bulk solution. Steric constraints, functional group positioning, and sequestration from other molecules can enforce reactivity and selectivity that is impossible when simpler catalysts are employed.[8, 13] Early work using crown ethers, cryptands, and cyclodextrins demonstrated the ability of molecular hosts to bind guests and influence chemical reactivity.[14-16] The development of host-mediated reactivity demands the creation of larger and more complex synthetic hosts, which in turn requires time-consuming multistep syntheses. As an alternative to covalent synthesis, chemists have designed large, well-defined structures that self-assemble from relatively simple subunits. Such supramolecular structures rely on weak and reversible interactions, such as hydrogen bonding or metal-ligand interactions, which are programmed into the subunits to form a single, thermodynamically stable assembly. This synthetic strategy provides access to complex structures in far fewer steps than traditional synthetic strategies, and has thus become a popular method for preparing large host assemblies.[10, 12, 17, 18]

Raymond and coworkers have developed a series of self-assembled supramolecular metal-ligand assemblies of M_4L_6 stoichiometry (M = Ga^{3+} (**1**), Al^{3+}, Fe^{3+}; L = *N,N′*-bis(2,3-dihydroxybenzoyl)-1,5-diaminonaphthalene).[19-22] The four trivalent metal atoms are located at the vertices of the tetrahedron, while naphthalene-based bis-bidentate catechol ligands span the edges, forming a *T*-symmetric, cavity-containing assembly (Figure 1). Strong mechanical coupling between the metal vertices through the ligands enforces self-assembly of a racemic mixture of the homochiral ΔΔΔΔ and ΛΛΛΛ configurations. The two enantiomers can be resolved and are configurationally stable.[23, 24]

A variety of monocationic guests ranging from simple alkylammonium cations to transition metal sandwich complexes are encapsulated inside of **1**, as well as neutral hydrophobic species such as alkanes.[25] Molecules that are highly solvated in water, such as dications and small monocations, are not encapsulated, while anionic molecules suffer from charge-repulsive interactions with the host that prevent their encapsulation. The 12- overall charge of **1** imparts water solubility, while the naphthalene rings of the ligand enclose the interior cavity, providing a hydrophobic environment for guest molecules. These properties allow water-labile cations such as ketone-derived iminium ions,[26] diazonium and tropylium ions,[27] and reactive phosphine-acetone adducts[27, 28] to be stabilized by encapsulation. While these cations are unstable, with very short lifetimes in aqueous solution, the polyanionic charge and hydrophobic cavity stabilize these species.

The properties of **1** that are summarized above have been exploited to develop reactions that occur inside the cavity of **1** with higher degrees of reactivity and/or selectivity than when the reaction is performed in bulk solution. For example, the acid-catalyzed hydrolysis of acetals and orthoformates is catalyzed by **1** in basic solution by lowering the pK_a of the encapsulated substrate.[29] Several encapsulated transition metal complexes can participate in stoichiometric and catalytic organometallic reactions in which **1** imposes strict limits on the size and shape of substrates that will react.[30-32]

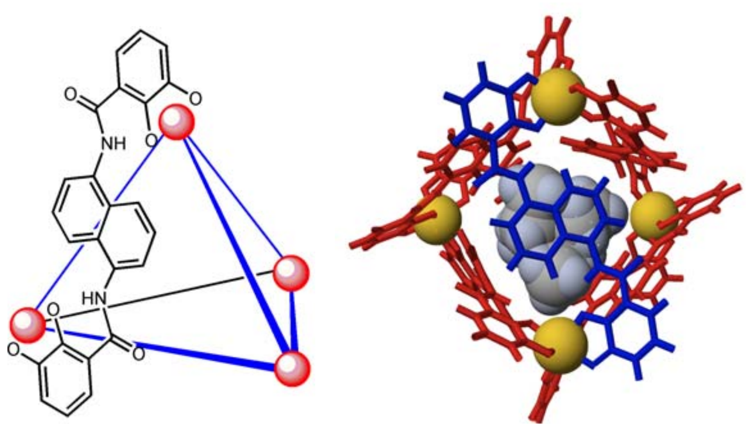

Figure 1. (Left) Schematic of the $[Ga_4L_6]^{12-}$ assembly (**1**); One ligand is shown for clarity. (Right) Model of **1** with a tetraethylammonium cation guest, viewed down the two-fold axis.

Pericyclic reactions are popular targets in supramolecular catalysis because encapsulation by itself can enforce the geometries necessary for enhanced reactivity, even in the absence of accelerating functional groups within the cavity. Diels-Alder reactions, for example, are particularly well suited for this mode of catalysis since binding of the diene and the dienophile into a constrictive environment dramatically increases the local concentration of these reactants. Rebek and coworkers reported the first example of a host-mediated Diels-Alder reaction, and several reports from the Fujita research group have utilized a metal-ligand host to accelerate the Diels-Alder reaction of unreactive dienes.[33-37] In both systems, product inhibition is observed unless the Diels-Alder adduct has a lower affinity for the host interior than the reactants.[34, 37] Thus, low levels of discrimination between the reactants and products of host-accelerated reactions are a major limitation of these reactions.

One strategy that can be used to circumvent this problem is the continuous conversion of product into a species that is not bound by the host. We have employed this approach in the catalysis of the sigmatropic rearrangement of allyl enammonium cations using the metal-ligand assembly **1** and performed a detailed study of the mechanism of this reaction.[38, 39] The 3-aza Cope rearrangement first converts an allyl enammonium cation to a γ,δ-unsaturated iminium cation via 3,3 sigmatropic rearrangement, which is then hydrolyzed to the corresponding aldehyde.[40, 41] This reaction is catalyzed by **1**, and rate enhancements of up to 854 times were measured.[38] Although the product iminium ion is encapsulated in **1**, hydrolysis converts this species to a neutral aldehyde that is much more weakly encapsulated, thereby allowing for catalytic turnover. The activation parameters for both the free and the assembly-mediated reaction were determined for several substrates, and while the enthalpies of activation were nearly identical, the entropies of activation for reactions of encapsulated guests were less negative compared to those occurring in free solution. This strongly suggests that a major component of the observed rate enhancement is the preorganization of the encapsulated substrate into a chair-like conformation that closely resembles the transition state of the sigmatropic rearrangement.

This hypothesis was confirmed by a NOESY experiment, which showed strong correlations between the two ends of the linear enammonium cation.[38]

Having investigated the catalysis of the aza Cope rearrangement of allyl enammonium ions using **1**, we were interested in extending the scope of this reaction to include propargyl-enammonium substrates (Scheme 1). These compounds react at a much slower rate than that of the allyl-vinyl substrates, necessitating elevated temperatures to obtain useful rates of reaction. For this reason, we sought to determine whether encapsulation within **1** would accelerate this more challenging reaction. Furthermore, having observed that rate enhancements are highly shape-selective in our original studies, we were interested in studying the propargyl compounds, which are not able to adopt the same conformations as the vinyl substrates. Here, we present an extension of this work to include the propargyl enammonium substrate class.

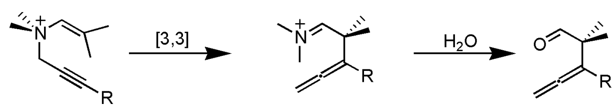

Scheme 1. General reaction scheme of the 3-aza Cope rearrangement. Starting from a propargyl enammonium cation, [3,3] sigmatropic rearrangement leads to an allenyl iminium cation, which then hydrolyzes to an allenyl aldehyde.

Results and Discussion

Encapsulation and Rate Acceleration. A range of propargyl enammonium tosylates with varying alkyl substituents at the alkyne terminus was prepared (Figure 2). Substrates were synthesized by alkylation of *N,N*-dimethylisobutenylamine with the corresponding propargyl tosylate in yields ranging from 15 to 89%. Crude yields were generally 80-90%, and the low yields reported for substrates **5**, **6**, **7**, and **10** were a result of inefficient recrystallizations necessary to obtain analytically pure material. Upon encapsulation in **1**, the guest resonances are shifted upfield 2-4 ppm due to the anisotropic ring current in the nearby naphthalene walls of **1**. Furthermore, encapsulation into the chiral interior of **1** renders enantiotopic guest protons diastereotopic. This typically affects the protons of a methylene group and the two *N*-methyl groups present in each substrate molecule. Host-guest complexes of compounds **2-9** are formed quantitatively in D_2O and DMSO-d_6, as determined by ^{1}H-NMR. Further evidence for these host-guest complexes was obtained by high-resolution electrospray mass spectrometry. Encapsulation occurs within minutes, and substrates can be ejected from the host interior by the addition of tetraethylammonium bromide, a strongly-binding guest. Guests bearing more sterically demanding *tert*-butyl (**10**), *n*-pentyl (**11**), and phenyl (**12**) substituents are not encapsulated, demonstrating that encapsulation of these substrates is highly size-dependent. It is noteworthy that among the four isomers bearing a butyl group at the alkyne terminus (**7-10**), only the *tert*-butyl substituted substrate **10** is excluded from the host interior. These results suggest that butyl-substituted compounds are only encapsulated if they possess a certain degree of conformational flexibility, and reflects the shape-selectivity of **1**.

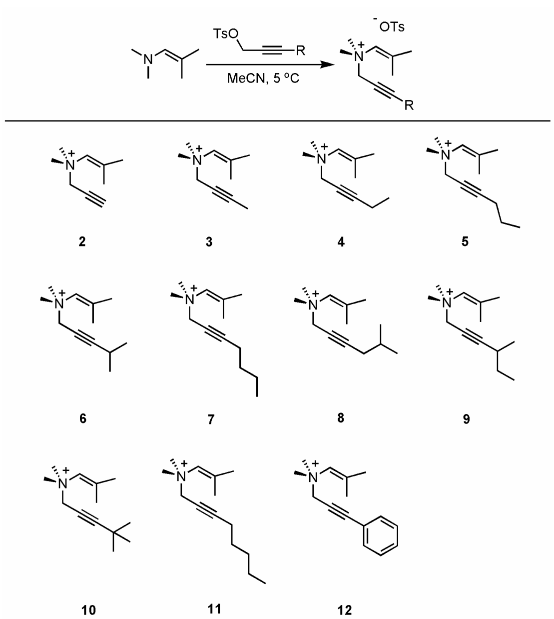

Figure 2. Synthesis of the propargyl enammonium substrates.

After demonstrating the scope of encapsulation, the rates of the aza Cope rearrangement/hydrolysis for both the free and encapsulated substrates were measured. Reactions were monitored by ^{1}H-NMR, and rates of reaction were based on the disappearance of starting material due to the insolubility of the product aldehydes in D_2O (product formation is observed by ^{1}H-NMR when wet DMSO-d_6 is used as the solvent). The reaction rates of encapsulated enammonium cations were measured using a stoichiometric amount of **1**, and the background reaction was monitored in the absence of **1**. Clean first-order disappearance of starting material was observed in both the encapsulated and the unencapsulated reactions, and the observed rate constants are shown in Table 1. For each substrate that was encapsulated by **1** (compounds **2-9**), encapsulation accelerated the rate of reaction up to two orders of magnitude over the free reaction. In the unencapsulated reaction, the substrates with larger groups at the alkyne terminus (**4-8**) react more slowly due to steric repulsion that disfavors the reactive, chair-like conformation required in the transition state. However, in the reaction of encapsulated substrates, the fastest rates were observed for the medium-sized substrates (**3-6**), while the largest and smallest compounds reacted more slowly. This "optimal fit" trend was also observed in our earlier work on allyl enammonium guests.

Table 1. Rate constants for background (k_{free}) and encapsulated (k_{encaps}) reactions (Measured at 60 °C in D_2O) and their rate accelerations

compound	R	k_{free} ($\times10^{-8}$ s^{-1})	k_{encaps} ($\times10^{-8}$ s^{-1})	k_{encaps}/k_{free}
2	H	62.4	237	4
3	Me	62.3	6200	100
4	Et	20.0	3670	184
5	*n*-Pr	19.5	1920	98
6	*i*-Pr	6.7	870	129
7	*n*-Bu	15.1	73	5
8	*i*-Bu	17.0	477	28
9	*s*-Bu	50.0	1150	23

Catalytic Kinetics. With the exception of **6**, the iminium rearrangement product is rapidly hydrolyzed to the corresponding aldehyde, leaving empty **1** behind. Previous studies have shown that the iminium hydrolysis step occurs outside the host cavity.[39] Encouraged by the regeneration of empty **1**, we explored the use of **1** as a catalyst for this reaction. Due to the relatively slow reaction rates of the reactions catalyzed by **1**, substrate **3**, having the fastest encapsulated rate of reaction (k_{encaps}), was used to study the kinetics of the catalytic system. Kinetic analysis of the catalytic reaction of substrate **3**

showed that when over 3 equivalents of substrate are present, the overall reaction is zeroth order in substrate (Figure 3). This suggests that the encapsulated starting material is the resting state of the catalyst and the rate-limiting step of the reaction is the sigmatropic rearrangement of the bound substrate, followed by rapid product release and binding an additional substrate molecule (Figure 4). Thus, the rate of reaction is dependent on the concentration of host-bound substrate, rather than the total concentration of substrate, leading to the equation: rate = k_2[**3** $\subset$ **1**] (where $\subset$ denotes encapsulation). Consistent with this rate law, under zeroth order conditions, the observed concentration of [**3** $\subset$ **1**] is invariant (Figure 3), confirming that host-bound starting material [**3** $\subset$ **1**] is the catalyst resting state. Using the experimentally determined concentration of [**3** $\subset$ **1**] and the observed rate of reaction, it is possible to determine the rate constant k_2 for this rate law. This first order rate constant is identical to the rate constant determined from the first order plot of the stoichiometric reaction of [**3** $\subset$ **1**]. Thus, the proposed rate law describes both the stoichiometric and the catalytic reaction. Throughout these experiments, the only encapsulated species present is host-bound starting material [**3** $\subset$ **1**]; The encapsulation of the iminium rearrangement product is never observed. Taken together with the kinetic profile of this reaction, we can conclude that **1** is a true catalyst in this reaction and does not suffer from product inhibition.

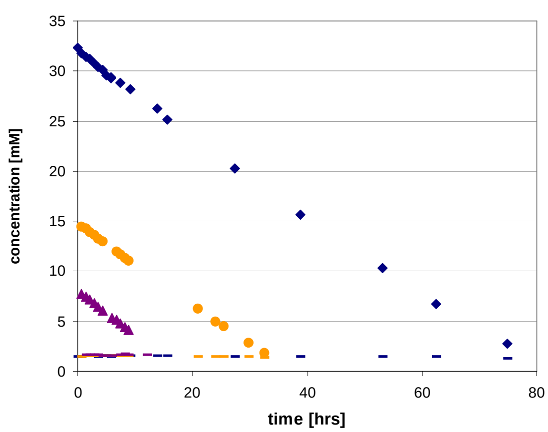

Figure 3. Concentration vs. time plots of the catalytic aza Cope rearrangement of **3**. Unbound starting material concentration: blue ◆, 19 equivalents of **3** with respect to **1**; orange ●, 9 equivalents of **3**; purple ▲, 4.5 equivalents of **3**.

Concentration of host-bound substrate [**3** ⊂ **1**]: Blue -, orange - and purple -, 19, 9, and 4.5 equivalents of **3** with respect to **1**, respectively.

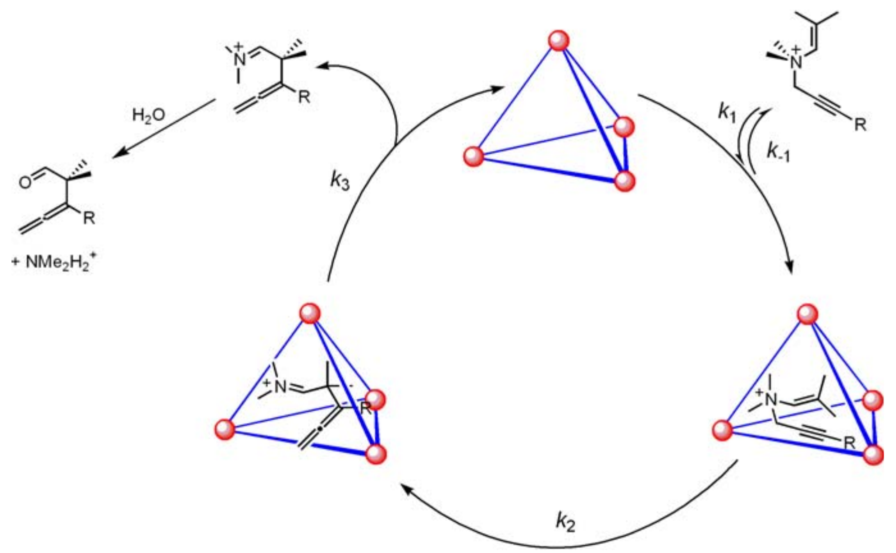

Figure 4. Proposed catalytic cycle for the propargyl 3-aza Cope rearrangement. The rearrangement of the encapsulated substrate (k_2) is rate determining.

Michaelis-Menten Analysis. In enzymatic catalysis, a substrate and enzyme are typically in a reversible equilibrium with an enzyme-substrate complex, and the conversion of enzyme-bound substrate into enzyme-bound product is rate determining. A consequence of this scenario is the observation of rate saturation at high substrate concentration. The Michaelis-Menten kinetic model is most frequently used to understand this type of enzymatic pathway.[42] The kinetic parameters of the catalyzed rearrangement for this model were determined from an Eadie-Hofstee plot of the substrate saturation curve of **3** (V_{max} = 1.2 x 10^{-4} mM s^{-1}, K_m = 0.67 mM, and k_{cat} = 7.0 x 10^{-5} s^{-1} where V_{max} is the maximum velocity of the reaction, K_m is the Michaelis constant, and k_{cat} is the turnover rate of the bound substrate).[43, 44] The calculated V_{max} is identical to the maximum measured velocity of the reaction under saturation conditions and the calculated k_{cat} is equal to the experimentally determined rate constant. In systems such as this where a fast pre-equilibrium is established prior to the catalytic step (k_1 and k_{-1} are much larger than k_2), the Michaelis constant K_m is essentially a dissociation constant. The K_m for **3** is larger than the K_d of NEt_4^+ (5.1 x 10^{-2} mM), but smaller than the K_d of NMe_4^+ (9.0

mM), which is consistent with competitive binding experiments in which **3** displaces [$NMe_4^+ \subset$ **1**], and NEt_4^+ displaces [**3** $\subset$ **1**].

A characteristic aspect of enzymatic catalysis is the inhibition of the enzyme active site with a suitable, non-reactive molecule whose binding is competitive with the substrate.[42] A bound inhibitor will exclude substrate from the active site thereby inhibiting the activity of the enzyme. If the binding of the substrate and the inhibitor is truly competitive, the inhibitor can be completely displaced if the substrate concentration is sufficiently high, and at infinite substrate concentration, the maximum reaction velocity (V_{max}) will be equal to that of the uninhibited reaction. To perform these experiments using **1**, several non-reactive alkylammonium guests were considered as competitive inhibitors. In previous work, we determined that ionic strength has no effect on the rate of reaction, so we were not concerned about any salt effects from added alkylammonium species.[39] The resonances of encapsulated NMe_4^+ overlap with those of encapsulated **3**, and the displacement of strongly-bound NEt_4^+ requires a large excess of **3**. Thus, both NMe_4^+ and NEt_4^+ are not suitable inhibitors for these experiments. The ^{1}H-NMR resonances of encapsulated NPr_4^+ are easily resolved from those of encapsulated **3** (Figure 5), and their binding constants are the same order of magnitude, making NPr_4^+ an ideal inhibitor for these experiments.

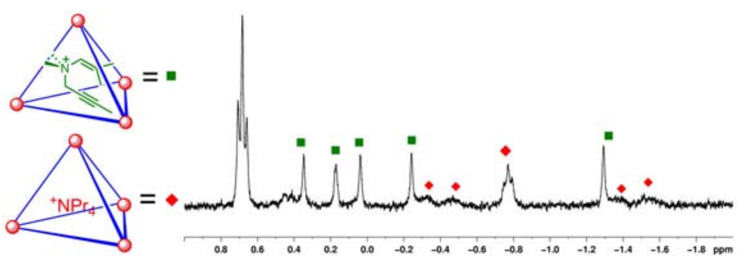

Figure 5. ^{1}H-NMR spectrum of a sample containing 1 equivalent each of **1**, substrate **3**, and NPr_4Br. Encapsulation is observed for both species.

Rate data under saturation conditions were collected in the presence of 4 and 10 equivalents of NPr_4^+ with respect to **1**. These data, together with the saturation data obtained in the absence of inhibitor, are shown in an Eadie-Hofstee plot (Figure 6), from which the relevant Michaelis-Menten parameters were determined.[43, 44] As expected, a larger excess of substrate is required to reach the maximum reaction velocity in the presence of inhibitor, but the same V_{max} is eventually achieved. These experiments clearly demonstrate that NPr_4^+ acts as a competitive inhibitor in this system, and show that the kinetic behavior of this system is comparable to our earlier studies of assembly-catalyzed orthoformate and acetal hydrolysis, as well as to the mode of action of enzymes.[29]

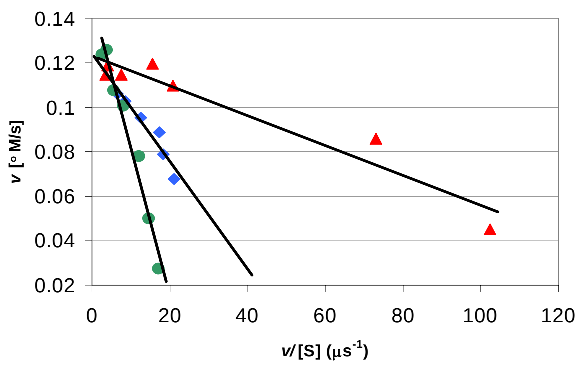

Figure 6. Eadie-Hofstee plot of inhibition data for the catalytic 3-aza Cope rearrangement of $[\mathbf{3} \subset Ga_4L_6]^{11-}$, using NPr_4^+ inhibitor. Red ▲, no inhibitor added; blue ◆, 4 equivalents NPr_4^+; green ●, 10 equivalents NPr_4^+.

Activation Parameters of the Catalytic Reaction. Our previous studies on the **1**-catalyzed aza Cope rearrangement revealed that lowered entropy of activation is responsible for rate enhancements over the background reaction. We sought to confirm that rate accelerations originated from the same entropic considerations in our system. Furthermore we wished to compare the change in entropy of activation of the propargyl enammonium substrates to the previously reported values.

Variable temperature kinetics of the catalyzed and uncatalyzed reaction of **3** were measured, and Eyring analysis of the resulting data provided activation parameters for both reactions. The activation parameters of the uncatalyzed rearrangement of **3** are $\Delta H^{\ddagger}$ = 23(3) kcal/mol and $\Delta S^{\ddagger}$ = -19(4) eu. The highly negative $\Delta S^{\ddagger}$ is a common feature of 3,3 sigmatropic rearrangements, and it reflects the organized transition state that the molecule must adopt in this reaction. The $\Delta S^{\ddagger}$ for this reaction is more negative than that measured for analogous allyl enammonium species, which accounts for the lower reactivity of the propargyl systems in the aza Cope rearrangement.[38] In general, however, the $\Delta S^{\ddagger}$ of the 3,3 sigmatropic rearrangment of 1,5-eneynes is not more negative than the $\Delta S^{\ddagger}$ of corresponding 1,5 dienes, and no clear trend in the activation parameters between these two classes of compounds has been identified.[45]

The activation parameters for the catalyzed rearrangement of **3** are are $\Delta H^{\ddagger}$ = 26(5) kcal/mol and $\Delta S^{\ddagger}$ = +2.8(9) eu. The $\Delta S^{\ddagger}$ differs by more than 20 eu from that of the background rearrangement, a dramatic change that strongly suggests that **1** selectively binds a preorganized, reactive conformations of the substrate. The bound substrate has fewer degrees of freedom in the confines of the assembly, and cannot adopt the conformation that would be lowest in energy for the unencapsulated molecule. The difference in the enthalpy of activation between the two reactions is within error, so it is clear that the entropic component of this reaction determines the observed rate enhancements.

Conclusion

In summary, we have demonstrated that a supramolecular metal-ligand assembly catalyzes the aza Cope rearrangement of propargyl enammonium cations. While classical catalysis of such sigmatropic rearrangements typically requires Lewis or Brønsted acid, substrate encapsulation within the confined host interior enforces a reactive conformation that accelerates the rates of rearrangement by up to 184 times. Consistent with this explanation, the determination of the activation parameters for the host-catalyzed and uncatalyzed reactions reveals that rate enhancements are due to a more positive $\Delta S^{\ddagger}$ for rearrangement in the catalytic reaction. The catalytic reaction obeys the Michaelis-Menten model of enzyme kinetics, and competitive inhibition of this reaction can be observed using NPr_4^+, a non-reactive guest. These studies demonstrate how supramolecular hosts are able to act as enzyme mimics in the catalysis of challenging reactions under mild, aqueous conditions. While Nature is able to catalyze a large number of chemical reactions using enzymes, synthetic chemists have only just begun to realize the potential of synthetic hosts in the catalysis of chemical reactions. As new supramolecular hosts are developed and their properties understood, we anticipate that many new examples of supramolecular catalysis will be discovered.

Experimental Section

General Considerations. Unless otherwise noted, reactions and manipulations were performed using standard Schlenk and high-vacuum techniques, and done at room temperature, unless otherwise noted. Glassware was dried in an oven at 150 °C overnight or flame-dried under vacuum prior to use. NMR spectra were obtained on Bruker Avance AV 300, AV 400, DRX 500, or AV-500 spectrometers. Chemical shifts are reported as δ in parts per million (ppm) relative to residual protonated solvent resonances. In the case of D_2O samples, ^{13}C shifts were referenced to an internal standard of CD_3OD.[46] Coupling constants are reported in Hz. IR spectra were measured neat on a Nicolet Avatar 370 FT-IR with a zinc selenide attenuated total reflective (ATR) accessory. Peak intensities are reported as (b) broad, (w) weak, (m) medium, or (s) strong. Only peaks in the functional group region (4000-1300 cm^{-1}) are reported.

Elemental analyses, low resolution fast atom bombardment, high resolution fast atom bombardment, and high resolution electrospray time of flight (TOF ESMS) mass spectrometry were performed at the University of California, Berkeley, Microanalytical Facility. Elemental analyses were performed on a Perkin-Elmer Series II CHNO/S analyzer. Reliable combustion analyses for the host-guest compounds were not possible due to varying amounts of solvent bound to the exterior of the assembly. Fast atom bombardment mass spectra were recorded on a Micromass ZAV2-EQ (magnetic sector) instrument. High resolution TOF ESMS of the host-guest complexes were recorded on a Waters QTOF API mass spectrometer equipped with a Z-spray source.

Unless otherwise noted, reagents were obtained from commercial suppliers and used without further purification. Anhydrous solvents were dried over activated alumina under nitrogen pressure and sparged with nitrogen before use.[47] *N,N*-dimethylisobutenylamine,[48] 4-methyl-2-hexynol[49], and 5-methyl-2-hexynol[50] were prepared according to published procedures.

General Procedure for Encapsulation Reactions. The potassium or sodium salt of **1** (3.0 mg, 0.85 μmol) and the enammonium tosylate (0.90 μmol) were combined in a vial and dissolved in 600 μL D_2O. The solution was transferred to an NMR tube and the spectrum was recorded within 20 minutes after dissolution. Samples for mass spectrometry were prepared in an identical fashion, using H_2O instead of D_2O. Samples were flushed with N_2 after mixing and mass spectra were obtained within 12 hours of sample preparation.

Analytical Data for Host-Guest Complexes, Prepared As Described Above.

K_{11}[2 ⊂ Ga_6L_6]. ^{1}H NMR (400 MHz, D_2O): δ 8.01 (d, ^3J = 7.6 Hz, 12H, Ar-*H*), 7.91 (d, ^3J = 6.8 Hz, 2H, OTs), 7.83 (d, ^3J = 8.4 Hz, 12H, Ar-*H*), 7.69 (d, , ^3J = 8.4 Hz, 2H, OTs), 7.31 (d, ^3J = 8.4 Hz, 12H, Ar-*H*), 7.09 (t, ^3J = 8.4 Hz, 12H, Ar-*H*), 6.77 (d, ^3J = 7.2 Hz, 12H, Ar-*H*), 6.62 (d, ^3J = 8.0 Hz, 12H, Ar-*H*), 2.37 (s, 3H, OTs), 2.06 (s, 1H, C*H*, encaps.), 0.52 (s, 1H, C*H*, encaps.), 0.48 (s, 1H, C*H*, encaps.), 0.28 (d, , ^4J = 16.0, 1H, C*H*, encaps.), -0.06 (s, 3H, CH_3, encaps.), -0.14 (s, 3H, CH_3, encaps.), -0.49 (s, 3H, CH_3, encaps.), -0.89 (s, 3H, CH_3, encaps.) ppm. TOF MS ES (-): (♦ denotes the host-guest species **K_{11}[2 ⊂ Ga_6L_6]**). Calc'd (found) *m/z:* $Ga_4C_{153}H_{103}N_{13}O_{36}K_8$ (♦ – $3K^+$)$^{3-}$ 1096.0198 (1096.0209), $Ga_4C_{153}H_{105}N_{13}O_{36}K_6$ (♦ – $5K^+$)$^{4-}$ 802.53 (802.53).

K_{11}[3 ⊂ Ga_6L_6]. ^{1}H NMR (400 MHz, D_2O): δ 8.04 (s, br, 12H, Ar-*H*), 7.82 (d, ^3J = 7.6 Hz, 12H, Ar-*H*), 7.69, (d, ^3J = 8.0 Hz, 2H, OTs), 7.35 (d, ^3J = 8.4 Hz, 2H, OTs), 7.30 (d, ^3J = 7.6 Hz, 12H, Ar-*H*), 7.07 (t, ^3J = 7.6 Hz, 12H, Ar-*H*), 6.76 (d, ^3J = 6.8 Hz, 12H, Ar-*H*), 6.61 (t, ^3J = 7.6 Hz, 12H, Ar-*H*), 2.37 (s, 3H, OTs), 1.95 (s, 1H, C*H*, encaps.), 0.65 (s, 3H, CH_3, encaps.), 0.57 (d, 1H, C*H*, encaps.), 0.51 (d, 1H, C*H*, encaps.), 0.19 (s, 6H, CH_3, encaps.), -0.18 (s, 3H, CH_3, encaps.), -1.10 (s, 3H, CH_3, encaps.) ppm. TOF MS ES (-): (♦ denotes the host-guest species **K_{11}[3 ⊂ Ga_6L_6]**). Calc'd (found) *m/z*:

$Ga_4C_{154}H_{105}N_{13}O_{36}K_8$ (♦ − $3K^+)^{3-}$ 1100.692 (1100.693), $Ga_4C_{154}H_{106}N_{13}O_{36}K_7$ (♦ − $4K^+)^{4-}$ 815.776 (815.775).

K_{11}[4 ⊂ Ga_6L_6]. ^1H NMR (400 MHz, D_2O): δ 8.04 (d, ^3J = 7.6 Hz, 12H, Ar-*H*), 7.76 (d, ^3J = 8.8 Hz, 12H, Ar-*H*), 7.70 (d, ^3J = 7.7 Hz, 2H, OTs), 7.38 (d, ^3J = 8.0 Hz, 2H, OTs), 7.33 (d, ^3J = 8.0 Hz, 12H, Ar-*H*), 7.03 (t, ^3J = 8.0 Hz, 12H, Ar-*H*), 6.78 (d, ^3J = 6.8 Hz, 12H, Ar-*H*), 6.62 (t, ^3J = 8.0 Hz, 12H, Ar-*H*), 2.40 (s, 3H, OTs), 1.76 (s, 1H, C*H*, encaps.), 0.94 (d, ^2J = 15.7 Hz, 1H, C*H*, encaps.), 0.75 (s, 3H, CH_3, encaps.), 0.67 (s, 3H, CH_3, encaps.), 0.40 (s, 3H, CH_3, encaps.), 0.09 (d, ^2J = 15.4 Hz, 1H, C*H*, encaps.), -0.52 (m, 2H, CH_2, encaps.), -1.02 (s, 3H, CH_3, encaps.), -1.06 (t, ^3J = 7.6 Hz, 3H, CH_3, encaps.) ppm. TOF MS ES (-): (♦ denotes the host-guest species **K_{11}[4 ⊂ Ga_6L_6]**). Calc'd (found) *m/z*: $Ga_4C_{155}H_{107}N_{13}O_{36}K_8$ (♦ − $3K^+)^{3-}$ 1105.364 (1105.364), $Ga_4C_{155}H_{108}N_{13}O_{36}K_7$ (♦ − $4K^+)^{4-}$ 819.280 (819.279).

K_{11}[5 ⊂ Ga_6L_6]. ^1H NMR (500 MHz, D_2O): δ 8.06 (d, ^3J = 7.5 Hz, 12H, Ar-*H*), 7.84 (d, ^3J = 9.0 Hz, 12H, Ar-*H*), 7.64 (d, ^3J = 7.5 Hz, 2H, OTs), 7.23 (d, ^3J = 7.5 Hz, 12H, Ar-*H*), 7.17 (d, ^3J = 7.5 Hz, 2H, OTs), 7.07 (t, ^3J = 8.0 Hz, 12H, Ar-*H*), 6.62 (d, ^3J = 6.5 Hz, 12H, Ar-*H*), 6.31 (t, ^3J = 7.5 Hz, 12H, Ar-*H*), 2.51 (s, 2H, CH_2, encaps.), 2.20 (s, 1H, C*H*, encaps.), 1.34 (s, 2H, CH_2, encaps.), 0.50 (q, ^3J = 12.8 Hz, 2H, CH_2, encaps.), 0.10 (s, 3H, CH_3, encaps.), 0.01 (s, 3H, CH_3, encaps.), -0.70 (s, 3H, CH_3, encaps.), -0.82 (s, 3H, CH_3, encaps.) ppm. TOF MS ES (-): (♦ denotes the host-guest species **K_{11}[5 ⊂ Ga_6L_6]**). Calc'd (found) *m/z*: $Ga_4C_{156}H_{109}N_{13}O_{36}K_8$ (♦ − $3K^+)^{3-}$ 1110.035 (1110.044), $Ga_4C_{156}H_{110}N_{13}O_{36}K_7$ (♦ − $4K^+)^{4-}$ 822.784 (822.781).

K_{11} [6 ⊂ Ga_6L_6]. ^1H NMR (500 MHz, D_2O): δ 8.07 (d, ^3J = 6.5 Hz, 12H, Ar-*H*), 7.72-7.67 (m, 14H, Ar-*H* + OTs), 7.36 (d, ^3J = 8.0 Hz, 12H, Ar-*H*), 7.29 (d, ^3J = 8.0 Hz, 12H, Ar-*H*), 7.01 (t, ^3J = 8.0 Hz, 12H, Ar-*H*), 6.74 (d, ^3J = 7.0 Hz, 12H, Ar-*H*), 6.59 (t, ^3J = 8.0 Hz, 12H, Ar-*H*), 1.70 (s, 1H, C*H*, encaps.), 1.19 (d, 1H, C*H*, encaps.), 1.10 (s, 3H, CH_3, encaps.), 1.03 (s, 1H, C*H*, encaps.), 0.73 (s, 3H, CH_3, encaps.), -0.36 (d, 1H, C*H*, encaps.), -1.03 (s, 3H, CH_3, encaps.), -1.48 (s, 3H, CH_3, encaps.), -1.60

(s, 3H, CH_3, encaps.) ppm. TOF MS ES (-): (♦ denotes the host-guest species **K$_{11}$[6 ⊂ Ga$_6$L$_6$]**). Calc'd (found) *m/z*: $Ga_4C_{156}H_{109}N_{13}O_{36}K_8$ (♦ – $3K^+)^{3-}$ 1110.036 (1110.009), $Ga_4C_{156}H_{110}N_{13}O_{36}K_7$ (♦ – $4K^+)^{4-}$ 822.784 (822.757).

Na$_{11}$[7 ⊂ Ga$_6$L$_6$]. ^{1}H NMR (500 MHz, D_2O): δ 8.06 (d, ^3J = 7.5 Hz, 12H, Ar-*H*), 7.75 (d, ^3J = 8.5 Hz, 12H, Ar-*H*), 7.70 (d, ^3J = 8.5 Hz, 2H, OTs), 7.36 (d, ^3J = 8.0 Hz, 2H, OTs), 7.33 (d, ^3J = 8.0 Hz, 12H, Ar-*H*), 6.99 (t, ^3J = 8.0 Hz, 12H, Ar-*H*), 6.79 (d, ^3J = 7.0 Hz, 12H, Ar-*H*), 6.62 (t, ^3J = 7.5 Hz, 12H, Ar-*H*), 2.01 (s, 1H, C*H*, encaps.), 1.49 (d, ^3J = 15 Hz, 1H, C*H*, encaps.), 1.24 (s, 3H, CH_3, encaps.), 0.66 (d, ^3J = 35.0 Hz, 6H, (CH_3)$_2$, encaps.), -0.05 (d, ^3J = 15.5 Hz, 1H, C*H*, encaps.), -0.206 (s, 2H, CH_2, encaps.), -0.958 (s, 3H, CH_3, encaps.), -1.042 (s, 3H, CH_3, encaps.), -1.42 (d, ^3J = 58.5 Hz, 2H, CH_2, encaps.), -1.71 (s, 2H, CH_2, encaps.) ppm. TOF MS ES (-): (♦ denotes the host-guest species **Na$_{11}$[7 ⊂ Ga$_6$L$_6$]**). Calc'd (found) *m/z*: $Ga_4C_{157}H_{111}N_{13}O_{36}Na_8$ (♦ – $3Na^+)^{3-}$ 1071.7742 (1071.7858), $Ga_4C_{157}H_{108}N_{13}O_{36}Na_7$ (♦ – $4Na^+)^{4-}$ 798.0843 (798.0863), $Ga_4C_{157}H_{108}N_{13}O_{36}Na_6$, (♦ – $5Na^+)^{5-}$ 633.8695 (633.8650).

K$_{11}$ [8 ⊂ Ga$_6$L$_6$]. ^{1}H NMR (500 MHz, D_2O): δ 8.06 (d, ^3J = 7.5 Hz, 12H, Ar-*H*), 7.75 (d, ^3J = 8.5 Hz, 12H, Ar-*H*), 7.70 (d, ^3J = 8.5 Hz, 2H, OTs), 7.36 (d, ^3J = 8.0 Hz, 2H, OTs), 7.33 (d, ^3J = 8.0 Hz, 12H, Ar-*H*), 6.99 (t, ^3J = 8.0 Hz, 12H, Ar-*H*), 6.79 (d, ^3J = 7.0 Hz, 12H, Ar-*H*), 6.62 (t, ^3J = 7.5 Hz, 12H, Ar-*H*), 2.90 (s, 1H, C*H*, encaps.), 1.15 (s, 2H, CH_2, encaps.), 0.62 (s, 3H, CH_3, encaps.), 0.51 (s, 3H, CH_3, encaps.), -0.45 (br, 1H, C*H*, encaps.), -1.0 (s, 3H, CH_3, encaps.), -1.3 – (-1.5) (br, 5H, CH_3 + CH_2, encaps.), -1.89 (br, 6H, 2 x CH_3, encaps.) ppm. TOF MS ES (-): (♦ denotes the host-guest species **K$_{11}$[8 ⊂ Ga$_6$L$_6$]**). Calc'd (found) *m/z*: $Ga_4C_{157}H_{112}N_{13}O_{36}K_7$ (♦ – $4K^+)^{4-}$826.288 (826.013), $Ga_4C_{157}H_{113}N_{13}O_{36}K_6$ (♦ – $5K^+$ + $H^+)^{4-}$ 816.799 (816.529), $Ga_4C_{157}H_{114}N_{13}O_{36}K_5$ (♦ – $6K^+$ + $2H^+)^{4-}$ 807.310 (807.776).

K$_{11}$ [9 ⊂ Ga$_6$L$_6$]. ^{1}H NMR (500 MHz, D_2O): δ 8.06 (d, ^3J = 7.5 Hz, 12H, Ar-*H*), 7.75 (d, ^3J = 8.5 Hz, 12H, Ar-*H*), 7.70 (d, ^3J = 8.5 Hz, 2H, OTs), 7.36 (d, ^3J = 8.0 Hz, 2H, OTs), 7.33 (d, ^3J = 8.0 Hz, 12H, Ar-*H*), 6.99 (t, ^3J = 8.0 Hz, 12H, Ar-*H*), 6.79 (d, ^3J = 7.0 Hz, 12H, Ar-*H*), 6.62 (t, ^3J = 7.5 Hz, 12H, Ar-*H*), -0.3 – (-1.1) (many overlapping peaks, encaps.), -1.25 (s, 3*H*, CH_3, encaps.), -1.55 (s, 2H, CH_2, encaps.), -1.79 (s, 6H, CH_3, encaps.), -1.8 – (-2.0) (broad overlapping peaks, encaps.), -2.18 (s, 6H, 2 x CH_3, encaps.) TOF MS ES (-): (♦ denotes the host-guest species $\mathbf{K_{11}[8 \subset Ga_6L_6]}$). Calc'd (found) *m/z*: $Ga_4C_{157}H_{112}N_{13}O_{36}K_7$ (♦ – $4K^+)^{4-}$826.288 (826.266), $Ga_4C_{157}H_{113}N_{13}O_{36}K_6$ (♦ – $5K^+$ + $H^+)^{4-}$ 816.799 (816.529), $Ga_4C_{157}H_{114}N_{13}O_{36}K_5$ (♦ – $6K^+$ + $2H^+)^{4-}$ 807.310 (807.786).

Kinetic Analyses of Enammonium Rearrangements. Kinetic analyses using an equimolar amount of **1** with respect to the enammonium substrate (Table 1) were performed in D_2O on a Bruker AVB 400 spectrometer. Due to the long reaction times associated with these reactions, kinetic runs were monitored by taking individual time points, and the reaction temperature was maintained outside the probe in an oil bath. The concentration of all samples was 15 mM; the solutions were buffered with 100 mM phosphate buffer and adjusted to pD 8.09. All samples were degassed by performing three vacuum/N_2 backfill cycles and sealed under vacuum to prevent the oxidation of **1**. The benzylic methyl peak of the tosylate counterion served as an internal standard for integration. The background reactions of unencapsulated substrates were monitored under the same conditions with regard to substrate concentration, buffer strength, and pD. For the majority of experiments, the decay of starting material was monitored using 2 scans with a delay time of 25 seconds and a 90° pulse of 8.15 μsec.

When the assembly **1** is subjected to three or more equivalents of any given propargyl enammonium substrate, significant precipitation occurs. For this reason DMSO-d_6 (20% by volume) was used as a cosolvent in experiments where substoichiometric amounts of **1** were used with respect to substrate. Kinetic runs using substoichiometric amounts of **1** were performed on Bruker AVB 400, AVQ 400, DRX 500 and AV 500 spectrometers. The concentration of all samples was 1.7 mM in **1**, and the mixed-solvent experiments were conducted without buffer.

Acknowledgment. We thank Dr. Dennis Leung for helpful discussions, Rudi Nunlist for assistance with NMR experiments, Dr. Ulla Andersen and Michael Pluth for assistance with mass spectrometry. This research is supported by the Director, Office of Science, Office of Basic Energy Sciences, and the Division of Chemical Sciences, Geosciences, and Biosciences of the U.S. Department of Energy at LBNL under Contract No. DE-AC02-05CH11231.

Supporting Information Available. Eyring plots for the determination of activation parameters for the rearrangement of **3** and **3** $\subset$ **1**, saturation data and inhibited saturation data for the catalyzed rearrangement of **3**, and characterization of new compounds. This material is available free of charge via the Internet at http://pubs.acs.org.

Works Cited:

1. Jencks, W. P., *Catalysis in Chemistry and Enzymology*. McGraw-Hill: New York, 1969.
2. Kirby, A. J. *Angew. Chem. Int. Ed. Engl.* **1996,** 35, 707-724.
3. Tramontano, A.; Janda, K. D.; Lerner, R. A. *Science* **1986,** 234, (4783), 1566-1570.
4. Borman, S. *Chem. Eng. News* **2004,** 82, (8), 35-39.
5. Hof, F.; Craig, S. L.; Nuckolls, C.; Rebek, J. **2002,** 41, 1448-1508.
6. Kleij, A. W.; Reek, J. N. H. *Chem. Eur. J.* **2006,** 12, 4218-4227.
7. Koblenz, T. S.; Wassenaar, J.; Reek, J. N. H. *Chem. Soc. Rev.* **2008,** 37, 247-262.
8. Lützen, A. *Angew. Chem. Int. Ed.* **2005,** 44, 1000-1002.
9. Motherwell, W. B.; Bingham, M. J.; Six, Y. *Tetrahedron* **2001,** 57, 4663-4686.
10. Oshovsky, G. V.; Reinhoudt, D. N.; Verboom, W. *Angew. Chem. Int. Ed.* **2007,** 46, (14), 2366-2393.
11. Sanders, J. K. M. *Chem. Eur. J.* **1998,** 4, (1378), 1378-1383.
12. Schmuck, C. *Angew. Chem. Int. Ed.* **2007,** 46, (31), 5830-5833.
13. Vriezema, D. M.; Aragone`s, M. C.; Elemans, J. A. A. W.; Cornelissen, J. J. L. M.; Rowan, A. E.; Nolte, R. J. M. *Chem. Rev.* **2005,** 105, 1445-1489.
14. Breslow, R.; Dong, S. D. *Chem. Rev.* **1998,** 98, 1997-2012.
15. Cram, D. J. *Angew. Chem., Int. Ed. Engl.* **1988,** 27, 1009-1020.
16. Lehn, J.-M. *Angew. Chem., Int. Ed. Engl.* **1988,** 27, 89-112.
17. Yeh, R. M.; Davis, A. V.; Raymond, K. N., Supramolecular systems: self-assembly. In *Comprehensive Coordination Chemistry II*, McCleverty, J. A.; Meyer, T. J., Eds. Elsevier Ltd.: Oxford, UK, 2004; pp 327-355.
18. Mimassi, L.; Guyard-Duhayon, C.; Rager, M. N.; Amouri, H. *Inorg. Chem.* **2004,** 43, 6644-6649.
19. Caulder, D. L.; Bruckner, C.; Powers, R. E.; Konig, S.; Parac, T. N.; Leary, J. A.; Raymond, K. N. *J. Am. Chem. Soc.* **2001,** 123, (37), 8923-8938.
20. Caulder, D. L.; Powers, R. E.; Parac, T. N.; Raymond, K. N. *Angew. Chem. Int. Ed.* **1998,** 37, 1840-1843.
21. Caulder, D. L.; Raymond, K. N. *J. Chem. Soc., Dalton Trans.* **1999**, 1185-1200.
22. Caulder, D. L.; Raymond, K. N. *Acc. Chem. Res.* **1999,** 32, 975-982.

23. Terpin, A. J.; Ziegler, M.; Johnson, D. W.; Raymond, K. N. *Angew. Chem. Int. Ed.* **2001,** 40, 157-160.
24. Ziegler, M.; Davis, A. V.; Johnson, D. W.; Raymond, K. N. *Angew. Chem. Int. Ed.* **2003,** 42, 665-668.
25. Biros, S. M.; Bergman, R. G.; Raymond, K. N. *J. Am. Chem Soc.* **2007,** 129, 12094-12095.
26. Dong, V. M.; Fiedler, D.; Carl, B.; Bergman, R. G.; Raymond, K. N. *J. Am. Chem. Soc.* **2006,** 128, 14464-14465.
27. Fiedler, D.; Pagliero, D.; Brumaghim, J. L.; Bergman, R. G.; Raymond, K. N. *Inorg. Chem.* **2004,** 43, 846-848.
28. Ziegler, M.; Brumaghim, J. L.; Raymond, K. N. *Angew. Chem. Int. Ed.* **2000,** 39, 4119-4121.
29. Pluth, M. D.; Bergman, R. G.; Raymond, K. N. *Science* **2007,** 316, 85.
30. Leung, D. H.; Bergman, R. G.; Raymond, K. N. *J. Am. Chem Soc.* **2006,** 128, 9781-9797.
31. Leung, D. H.; Bergman, R. G.; Raymond, K. N. *J. Am. Chem Soc.* **2007,** 129, 2746-2747.
32. Leung, D. H.; Fiedler, D.; Bergman, R. G.; Raymond, K. N. *Angew. Chem. Int. Ed.* **2004,** 43, 963-966.
33. Kang, J. M.; Hilmersson, G.; Santamaria, J.; Rebek, J. *J. Am. Chem. Soc.* **1998,** 120, (15), 3650-3656.
34. Kang, J. M.; Rebek, J. *Nature* **1997,** 385, 50-52.
35. Kang, J. M.; Santamaria, J.; Hilmersson, G.; Rebek, J. *J. Am. Chem. Soc.* **1998,** 120, (29), 7389-7390.
36. Nishioka, Y.; Yamaguchi, T.; Yoshizawa, M.; Fujita, M. *J. Am. Chem Soc.* **2007,** 129, 7000-7001.
37. Yoshizawa, M.; Tamaru, M.; Fujita, M. *Science* **2006,** 312, 251 - 254.
38. Fiedler, D.; Bergman, R. G.; Raymond, K. N. *Angew. Chem. Int. Ed.* **2004,** 43, 6748-6751.
39. Fiedler, D.; van Halbeek, H.; Bergman, R. G.; Raymond, K. N. *J. Am. Chem. Soc* **2006**.
40. Elkik, E.; Francesch, C., *Bull. Soc. Chim.* **1968,** 3, 903-910.
41. Opitz, G. *Justus Liebigs Ann. Chem.* **1961**, 122-132.
42. McKee, T.; McKee, J. R., *Biochemistry: The Molecular Basis of Life*. Third ed.; McGraw-Hill: New York, 2003.
43. Eadie, G. S. *J. Biol. Chem.* **1942,** 146, 85.
44. Hofstee, B. H. J. *Science* **1952,** 116, 329.
45. Viola, A.; MacMillan, J. H. *J. Am. Chem. Soc.* **1970,** 92, 2404.
46. Gottleib, H. E.; Kotlyar, V.; Nudelman, A. *J. Org. Chem.* **1997,** 62, 7512.
47. Alaimo, P. J.; Peters, D. W.; Arnold, J.; Bergman, R. G. *J. Chem. Educ.* **2001,** 78, 64.
48. Ellenberger, M. R.; Dixon, D. A.; Farneth, W. E. J., *J. Am. Chem. Soc.* **1981,** 103, 5377.
49. Corey, E. J.; Fuchs, P. L. *Tett. Lett.* **1972,** 36, 3769.
50. Capon, R. J.; Barrow, R. A. *J. Org. Chem.* **1998,** 63, 75-83.